

MixAR: Mixture Autoregressive Image Generation

Jinyuan Hu^{1,2*}Jiayou Zhang²Shaobo Cui³Kun Zhang^{2,4}Guangyi Chen^{2,4}¹Tsinghua University²Mohamed bin Zayed University of Artificial Intelligence (MBZUAI)³École Polytechnique Fédérale de Lausanne (EPFL)⁴Carnegie Mellon University

Abstract

Autoregressive (AR) approaches, which represent images as sequences of discrete tokens from a finite codebook, have achieved remarkable success in image generation. However, the quantization process and the limited codebook size inevitably discard fine-grained information, placing bottleneck on fidelity. Motivated by this limitation, recent studies have explored autoregressive modeling in continuous latent spaces, which offers higher generation quality. Yet, unlike discrete tokens constrained by a fixed codebook, continuous representations lie in a vast and unstructured space, posing significant challenges for efficient autoregressive modeling. To address these challenges, we introduce **MixAR**, a novel framework that leverages mixture training paradigms to inject discrete tokens as prior guidance for continuous AR modeling. MixAR is a factorized formulation that leverages discrete tokens as prior guidance for continuous autoregressive prediction. We investigate several discrete-continuous mixture strategies, including self-attention (DC-SA), cross-attention (DC-CA), and a simple approach (DC-Mix) that replaces homogeneous mask tokens with informative discrete counterparts. Moreover, to bridge the gap between ground-truth training tokens and inference tokens produced by the pre-trained AR model, we propose Training–Inference Mixture (TI-Mix) to achieve consistent training and generation distributions. In our experiments, we demonstrate a favorable balance of the DC-Mix strategy between computational efficiency and generation fidelity, and consistent improvement of TI-Mix.

1. Introduction

Recent successes in large language models (LLMs) have demonstrated the remarkable capability of the autoregressive framework in sequence modeling [1, 2, 9, 14]. Moti-

*This work was done during Jinyuan Hu’s visit to Mohamed bin Zayed University of Artificial Intelligence (MBZUAI).

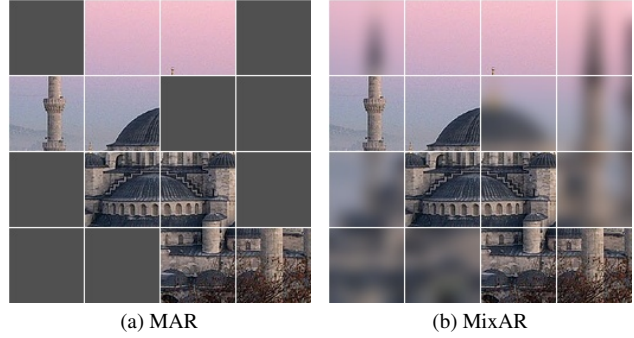


Figure 1. **Intuition behind MixAR.** Compared with the traditional masked autoregressive (MAR) strategy that predicts the full image from only a subset of visible patches (a), MixAR reconstructs the image from a partially degraded yet still informative version (b). This design provides richer contextual cues and captures fine-grained details more effectively.

vated by this success, a growing line of research has adapted AR modeling to image generation [6, 10, 12, 17, 19, 24, 27]. Mainstream AR methods use discrete-valued tokens as input contexts and generation targets, as discrete modeling can be efficiently optimized, such as using the cross-entropy loss. However, to compress an image into a sequence of discrete tokens, the quantization step is indispensable, which maps continuous latent vectors to discrete codewords in a finite codebook [11, 15, 23, 26, 29], inevitably causing information loss. Moreover, the representational capacity of these models is fundamentally limited by the codebook size, while enlarging the codebook often leads to optimization difficulties. These constraints impose an intrinsic upper bound on the fidelity achievable by discrete autoregressive models.

In contrast, recent studies have explored continuous autoregressive models that directly learn the joint distribution of continuous latents without quantization [13]. Despite their conceptual appeal, these methods face optimization challenges, as continuous representations reside in a vast and unstructured space, unlike their discrete counterparts

constrained by a codebook. This creates a fundamental dilemma: discrete models are easier to train but inherently lossy, while continuous models offer higher fidelity yet suffer from training inefficiency.

To address this challenge, we take inspiration from classic continuous regression methods [20, 28], which mitigate optimization difficulties by performing a coarse discrete classification prior to continuous regression. This cascaded refinement paradigm has also been proven effective in other vision tasks like object detection [16] and pose estimation [5]. We hypothesize that a similar factorization can also benefit image generation. Specifically, rather than directly modeling the continuous latent distribution in a single stage, we propose to decouple the process into two complementary components: a discrete module that first predicts discrete tokens (formulated as a classification problem), and a continuous module that generates high-fidelity continuous latents under the guidance of these classification results (formulated as a regression problem). This factorization combines the stability of discrete training with the expressive power of continuous modeling, resolving the trade-off between optimization efficiency and fidelity.

Motivated by this insight, we propose **MixAR**, a novel framework that leverages a mixture of discrete and continuous tokens to incorporate guidance from discrete representations. Instead of directly learning the joint distribution of continuous latents [13], MixAR adopts factorized formulation that models the conditional continuous distribution given discrete variables. In this formulation, off-the-shelf discrete AR models are employed to capture the distribution over discrete tokens, while the continuous component is learned through a masked autoregressive strategy guided by the discrete variables. As shown in Figure 1, the standard MAR framework replaces masked regions with a single, non-informative mask token, predicting the full image from visible patches only. In contrast, DC-Mix substitutes these regions with discrete tokens that preserve partial semantic and structural information, enabling reconstruction from a partially degraded input rather than entirely missing regions.

Furthermore, we investigate several strategies for injecting discrete guidance into the continuous AR model, including self-attention (DC-SA), cross-attention (DC-CA), and a direct mixture approach (DC-Mix). Specifically, DC-SA and DC-CA utilize discrete tokens as prefix inputs and incorporate their guidance into continuous modeling through self- and cross-attention mechanisms, respectively. DC-Mix, rather than adding prefix discrete tokens, directly replaces homogeneous, non-informative mask tokens with semantically rich discrete context. Interestingly, we found that DC-Mix introduces no additional parameters yet achieves fidelity comparable to methods using prefix tokens. In practice, if absolute performance is the prior-

ity and a higher training cost is acceptable, DC-SA is the most effective choice, as it utilizes all tokens for guidance. For computationally constrained settings, we recommend DC-Mix, which provides a favorable trade-off between efficiency and fidelity.

In addition, we find that incorporating discrete guidance inevitably introduces a distribution mismatch between the ground-truth discrete tokens used during training and the model-generated tokens encountered at inference. To address this universal issue, we introduce Training–Inference Mixture (TI-Mix), a simple yet broadly applicable plug-in technique that gradually interpolates between ground-truth and generated discrete tokens during training. Specifically, we jointly mix the continuous contextual tokens, ground-truth discrete tokens, and generated discrete tokens from the pre-trained discrete AR model. During training, we progressively replace ground-truth priors with generated ones, allowing the continuous AR model to gradually adapt to realistic inference conditions.

Through extensive experiments, we demonstrate that MixAR outperforms the standard MAR consistently on both model sizes. By systematically analyzing different guidance strategies, we find that DC-Mix achieves an attractive balance between computational efficiency and generation fidelity, while TI-Mix further improves generation quality by reducing the training–inference discrepancy. As illustrated in Figure 2, MixAR produces substantially more detailed and coherent images than MaskBit, highlighting the advantage of leveraging discrete priors to guide continuous latent prediction.

In summary, our contributions are as follows:

- We reformulate continuous autoregressive modeling as a **factorized process**, which incorporates the priors of discrete tokens into the continuous space, achieving better optimization efficiency and generation fidelity.
- We systematically compare different guidance strategies, such as DC-SA and DC-CA, and **DC-Mix**, and find that the direct mixture of DC-Mix achieves a favorable trade-off between efficiency and fidelity.
- We introduce **TI-Mix** to gradually blend ground-truth and generated discrete tokens during training, reducing the distribution mismatch between training and inference.

2. Related Work

2.1. Discrete Autoregressive Image Generation

Discrete autoregressive modeling has been widely adopted for image generation [3, 6, 10, 12, 17, 19, 24], inspired by the advances of large language models in sequence modeling. These methods quantize images into sequences of discrete tokens (e.g., via VQ-VAE [23] or VQ-GAN [10]) and model their joint distribution using cross-entropy loss. Existing approaches can be broadly divided



Figure 2. **MixAR vs Maskbit** Top: Images generated by Maskbit [24]. Bottom: Images generated by our MixAR-L model conditioned on the discrete tokens produced by Maskbit, demonstrating significant improvements in generation quality.

into two paradigms: the next-token prediction paradigm and the masked autoregressive paradigm, depending on how conditional dependencies are formulated and tokens are generated during inference.

The next-token paradigm, derived from GPT-style language modeling [4], predicts tokens sequentially [10, 17, 19], while the masked autoregressive paradigm, inspired by BERT-style masked prediction [8], predicts multiple masked tokens in parallel, generating a subset at each step until all tokens are produced [3, 6, 12, 24]. Despite their differences, both paradigms fundamentally rely on quantization [10, 15, 23, 26, 29] to obtain discrete representations, making them subject to the information loss and limited representational capacity imposed by finite codebooks. These constraints motivate the exploration of continuous autoregressive modeling, which seeks to bypass quantization by directly learning in continuous latent spaces.

2.2. Continuous Autoregressive Image Generation

Continuous autoregressive (AR) modeling aims to bypass the quantization bottleneck of discrete methods by directly learning dependencies in continuous latent spaces. The pioneering work MAR [13] establishes the first strong continuous AR baseline by applying masked autoregressive modeling to continuous latents and refining predictions with a diffusion-based denoising head. By eliminating codebook quantization, MAR demonstrates the potential of continuous representations to achieve higher fidelity and richer generative capacity. Following MAR, several subsequent works explore alternative formulations of continuous autoregression. For example, FlowAR [18] incorporates flow-based parameterizations to better capture complex latent distributions, while HART [21] leverages hybrid trans-

former-diffusion architectures to improve stability and scalability. Although these methods introduce valuable design choices, continuous AR models as a whole remain challenging to optimize due to the vast, unstructured nature of continuous latent spaces. Our motivation is that the expressive potential of continuous representations can be more effectively realized through a factorized formulation that introduces discrete priors, along with mixture strategies that provide more stable and informative guidance during autoregressive prediction.

3. Method

In this section, we first present the preliminaries of continuous autoregressive modeling (MAR). We then illustrate how to leverage factorization to decompose continuous modeling into a discrete autoregressive component and a conditional module that generates continuous tokens based on discrete ones. Finally, we discuss how to inject discrete tokens as guidance for continuous generation and how to bridge the gap between ground-truth training tokens and inference tokens produced by the pre-trained AR model.

3.1. Masked Autoregressive Model (MAR)

Tokenization. Given an image $I \in \mathbb{R}^{H \times W \times 3}$, the discrete AR models first utilize a pre-trained tokenizer such as VQVAE to encode I into latent representations $I' \in \mathbb{R}^{h \times w \times d}$, where h, w, d denote the latent height, width, and channel dimensions respectively. The latent feature map I' is then reshaped into a sequence of $N = h \times w$ latents

$$X_d = [x_d^1, x_d^2, \dots, x_d^N],$$

where each $x_d^i \in \mathbb{R}^d$ is a discrete token.

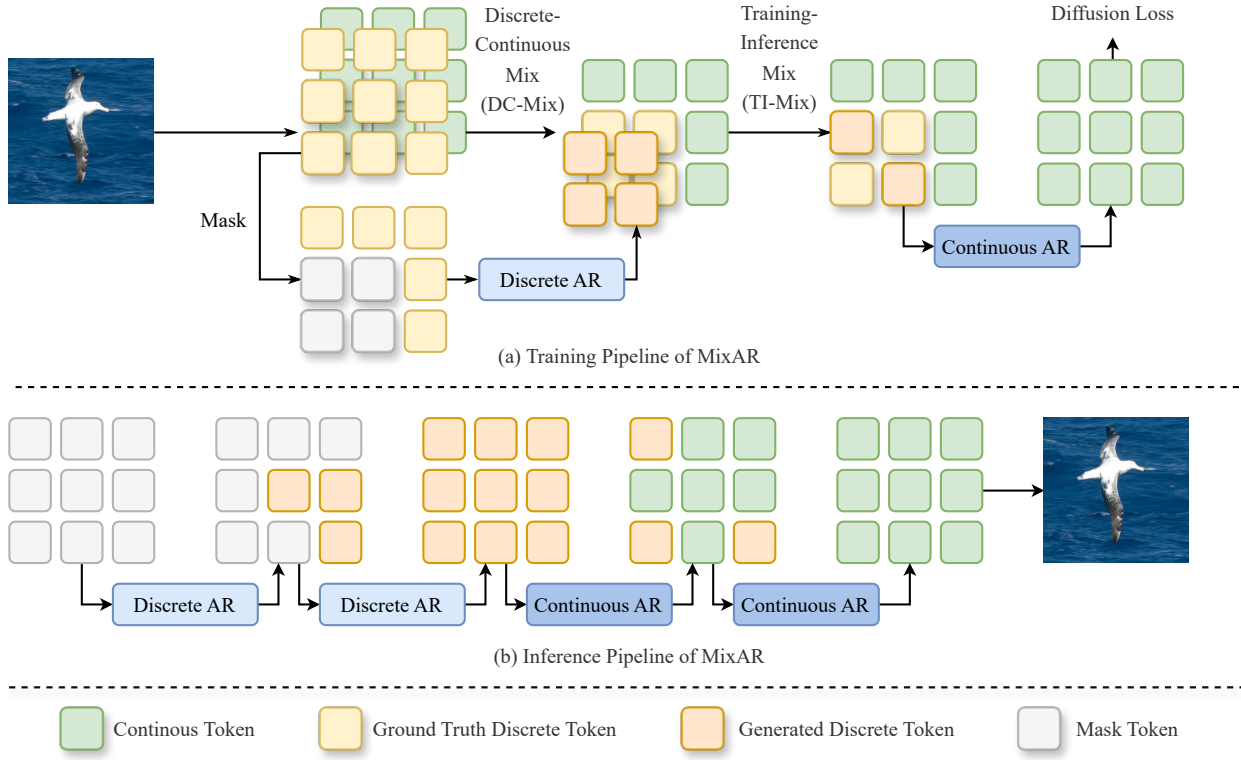


Figure 3. **Overview of the training and inference pipeline of MixAR.** During training, we first mix ground truth continuous and discrete tokens with DC-Mix, followed by TI-Mix that replaces a certain portion of ground truth discrete tokens with generated ones. The continuous AR model then predicts the ground-truth continuous tokens given the mixed tokens, optimized by diffusion loss. During inference, we first generate discrete tokens with a pretrained autoregressive model and use them to guide the continuous autoregressive model to generate more information-rich continuous tokens.

Autoregressive modeling. The joint probability of all tokens is then factorized autoregressively as

$$p(\mathbf{x}_d) = \prod_{i=1}^N p(x_d^i | x_d^{<i}), \quad (1)$$

and are typically trained using the cross-entropy loss:

$$\mathcal{L}_{\text{AR}} = - \sum_{i=1}^N \log p_\theta(x_d^i | x_d^{<i}). \quad (2)$$

While next-token prediction models effectively capture long-range dependencies, the strict autoregressive ordering limits flexibility in modeling two-dimensional spatial relationships.

Masked autoregressive paradigm. In contrast, the masked autoregressive paradigm relaxes the sequential dependency by predicting a subset of masked tokens in parallel, conditioned on the visible ones. During training,

random binary mask $M = [m^1, m^2, \dots, m^N]$ is applied, and the model predicts all masked positions with a single forward pass:

$$\mathcal{L}_{\text{MaskedAR}} = - \sum_{i: m^i=1} \log p_\theta(x_d^i | X_d^{<i}), \quad (3)$$

where $X_d^{<i}$ denotes the sequence with its i -th token masked.

At inference time, the model iteratively refines the masked positions over autoregressive steps t :

$$\hat{x}_d^{i,(t)} \sim p_\theta(x_d^i | \hat{X}_d^{<i,(t-1)}), \quad (4)$$

until all tokens are updated. $\hat{x}_d^{i,(t)}$ denotes that the generated new tokens at the masked position with $i : m^i = 1$ at step t . $\hat{X}_d^{<i,(t-1)}$ represent the generated sequence from step $t-1$ with i -th token masked.

Compared with next-token prediction, masked autoregression naturally aligns with the two-dimensional structure of images: each prediction step conditions on a set of spatially distributed visible tokens instead of a rigid 1D prefix.

This flexible conditioning enables the model to better capture local and global spatial dependencies, making it particularly suited for our discrete-continuous mixture formulation. Our MixAR is implemented on top of this paradigm.

Continuous masked autoregression. Based on this masked autoregressive paradigm, MAR [13] proposed to build continuous autoregression. Given the continuous tokens $X_c = [x_c^1, x_c^2, \dots, x_c^N]$ from a variational autoencoder (VAE), MAR selects $\lceil r \cdot N \rceil$ tokens and replaces them with a learnable mask token, where r denotes the masking ratio sampled from a pre-defined distribution $p(r)$. The masked sequence is then fed into a transformer-based model, which predicts the ground-truth latent x_c^i at each masked position i based on the context, following the masked autoregressive paradigm.

Diffusion losses. To effectively handle the high complexity of continuous distributions, MAR introduces a lightweight diffusion head that refines the autoregressive prediction into final latent estimates. Formally, given the backbone output z^i at each masked position i , the diffusion head learns to denoise a noise-corrupted version of the target latent $x_c^{i,t}$ under the standard denoising objective:

$$\mathcal{L}(z^i, x_c^i) = \mathbb{E}_{\varepsilon, t} \left[\left\| \varepsilon - \varepsilon_\theta(x_c^{i,t} \mid t, z^i) \right\|^2 \right], \quad (5)$$

where $\varepsilon \sim \mathcal{N}(0, I)$, t denotes the diffusion timestep, and ε_θ denotes the diffusion head. Although the diffusion loss benefits optimization, continuous autoregressive modeling remains challenging due to the complexity of the representation space, motivating us to further facilitate it with a mixture training mechanism.

3.2. Factorization Perspective

Different from MAR, which directly models the joint distribution of continuous latents $p_\theta(X_c)$ in an unconditional manner, our MixAR framework adopts a factorized formulation that leverages an auxiliary discrete representation as an informative prior. Specifically, we first employ a pre-trained discrete autoregressive model to approximate the discrete joint distribution $p_\phi(X_d)$, and then learn a conditional model over continuous latents:

$$p_\theta(X_c \mid X_d) = \prod_{i=1}^N p_\theta(x_c^i \mid x_c^{<i}, X_d), \quad (6)$$

where X_d provides structured guidance derived from the learned discrete manifold. Such guidance offers an explicit prior for the continuous autoregressive model, substantially reducing the complexity of directly modeling the full continuous latent space and making continuous generation more tractable.

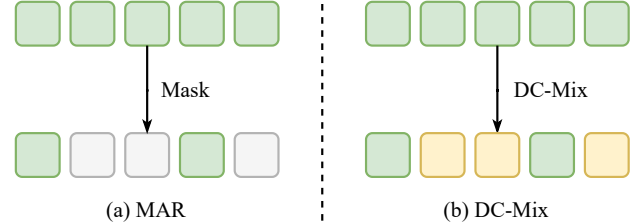


Figure 4. Comparison between MAR and DC-Mix. (a) In MAR, masked positions are replaced by a single meaningless mask token before prediction. (b) In contrast, DC-Mix pads masked regions with informative discrete tokens that carry semantic and structural cues, making the prediction easier with no additional computation cost. The legend follows the same convention as Figure 3.

3.3. Discrete-Continuous Mixture

The MixAR framework begins with **Discrete–Continuous Mixture (DC-Mix)**, a novel guidance strategy for injecting discrete conditional signals into continuous modeling. We employ both pretrained variational autoencoder (VAE) [25] and vector-quantized VAE (VQ-VAE) [24] to extract two complementary representations:

$$\mathbf{x}_c = \text{VAE}(I), \quad \mathbf{x}_d = \text{VQVAE}(I). \quad (7)$$

Here, $\mathbf{x}_c \in \mathbb{R}^{h \times w \times d_c}$ denotes the continuous representations, while $\mathbf{x}_d \in \mathbb{R}^{h \times w \times d_d}$ represents the discrete ones.

During training, both are flattened into sequences $X_c = [x_c^1, x_c^2, \dots, x_c^N]$ and $X_d = [x_d^1, x_d^2, \dots, x_d^N]$, where $N = h \times w$. Following the masked autoregressive algorithm, we randomly select $N' = \lceil r \cdot N \rceil$ positions $[k_1, k_2, \dots, k_{N'}]$ and generate a mask sequence $M = [m^1, m^2, \dots, m^N]$ where

$$m^i = \begin{cases} 1, & i \in [k_1, k_2, \dots, k_{N'}], \\ 0, & \text{otherwise.} \end{cases} \quad (8)$$

As illustrated in Figure 3, instead of replacing the masked elements x_c^i with a homogeneous learnable mask token as MAR, we substitute each with its discrete counterpart x_d^i (as shown in Figure 4), producing a mixed sequence $\tilde{X} = [\tilde{x}^1, \tilde{x}^2, \dots, \tilde{x}^N]$ defined by

$$\tilde{x}^i = \begin{cases} x_d^i, & m^i = 1, \\ x_c^i, & m^i = 0. \end{cases} \quad (9)$$

The mixed sequence \tilde{X} is then fed into the transformer-based backbone model, which outputs predictions z^i for each masked position. Each z^i is used to reconstruct the corresponding x_c^i via a diffusion head, following the MAR setting described in Section 3.1.

Comparison with other guidance strategies. We also tried other strategies to inject the guidance, such as the

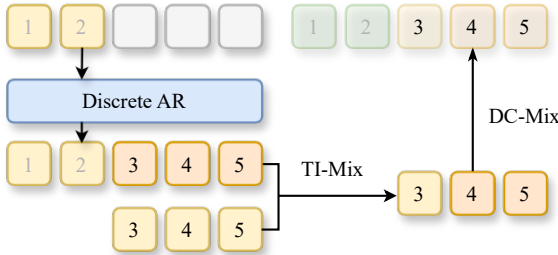


Figure 5. **Illustration of TI-Mix.** As shown in Figure 4, without TI-Mix, only ground truth discrete tokens are used as guidance during training, which is different from the generated tokens used in inference. In contrast, TI-Mix uses a mixture of ground truth and generated discrete tokens as guidance during training, effectively mitigating the distribution gap. Here the positions 3,4,5 form the masked region shared by ground truth discrete and continuous tokens. The legend follows the same convention as Figure 3.

self-attention (DC-SA) and cross-attention (DC-CA). DC-SA takes all discrete tokens $X_d = [x_d^1, x_d^2, \dots, x_d^N]$ as prefix contextual tokens. In the masked autoregressive process, all discrete tokens are used as seen tokens in self-attention to recover the masked tokens, with the $2 \times$ sequence length. While DC-CA takes all discrete tokens $X_d = [x_d^1, x_d^2, \dots, x_d^N]$ as prefix contextual memory and calculate as cross attention between these discrete tokens and continuous sequences. Unlike prefix-based self-attention, which expands the input length from N to $2N$ and thus increases attention complexity from $O(N^2)$ to $O((2N)^2) = 4O(N^2)$, DC-Mix preserves the original sequence length. Compared with cross-attention, whose theoretical complexity remains $O(N^2)$, DC-Mix still offers practical efficiency gains by avoiding additional projection parameters and extra attention operations required at every block, thereby reducing both computation and memory overhead. Despite its lightweight design, we demonstrate that DC-Mix achieves generation fidelity comparable to these more complex guidance strategies, making it an efficient and scalable solution for continuous autoregressive modeling.

3.4. Training-Inference Mixture (TI-Mix)

When discrete guidance is introduced into continuous modeling, the tokens used at inference time, denoted as $\hat{X}_d = [\hat{x}_d^1, \hat{x}_d^2, \dots, \hat{x}_d^N]$, are generated by the pretrained discrete AR model rather than taken from ground truth $X_d = [x_d^1, \dots, x_d^N]$. This distributional discrepancy ($p(\hat{X}_d) \neq p(X_d)$) leads to a training–inference gap. We employ TI-Mix to mitigate this gap.

Given a sequence of discrete tokens $X_d = [x_d^1, x_d^2, \dots, x_d^N]$, the binary mask $M = [m^1, m^2, \dots, m^N]$

used for DC-Mix, a pretrained AR model g_M in the masked autoregressive paradigm and its learned mask token t_m , we first construct the masked sequence

$$x_d^{i*} = \begin{cases} t_m, & m^i = 1, \\ x_d^i, & m^i = 0. \end{cases} \quad (10)$$

Feeding $X'_d = [x_d'^1, \dots, x_d'^N]$ into g_M yields the model prediction

$$\hat{X}_d = [\hat{x}_d^1, \hat{x}_d^2, \dots, \hat{x}_d^N] = g_M(X'_d), \quad (11)$$

where \hat{x}_d^i is generated only for masked region (where $m^i = 1$) and keeps the same as original x_d^i for the unmasked region (where $m^i = 0$). Now for the masked region, we have both ground truth and generated discrete tokens. Then TI-Mix is done by partially replace ground-truth tokens in the masked region with generated ones, as shown in 5. Let $\lambda \in [0, 1]$ denotes the ratio of ground-truth guidance, and a random variable $\rho^i \sim \mathcal{U}(0, 1)$ for each position i . The final mixed sequence $\tilde{X}_d = [\tilde{x}_d^1, \tilde{x}_d^2, \dots, \tilde{x}_d^N]$ is defined by

$$\tilde{x}_d^i = \begin{cases} \tilde{x}_d^i, & m^i = 1 \text{ and } \rho^i < \lambda, \\ \hat{x}_d^i, & m^i = 1 \text{ and } \rho^i \geq \lambda, \\ x_d^i, & m^i = 0. \end{cases} \quad (12)$$

The tokens in the masked region of \tilde{X}_d serve as new guidance for continuous modeling. By monotonically decreasing λ during training, the model gradually transitions from ground-truth to generated guidance, improving its adaptation to realistic inference conditions.

4. Experiments

We conduct all experiments on the ILSVRC-2012 ImageNet dataset, using the commonly adopted 256×256 resized version (ImageNet-256) [7]. Each image is pre-tokenized using two complementary tokenizers: a discrete tokenizer from Maskbit [24] and a continuous tokenizer based on the VA-VAE framework proposed in LightningDiT [25]. We use Maskbit [24] as our discrete AR model. The architecture of the continuous AR model is adopted from MAR [13].

4.1. Comparison with MAR

A comprehensive quantitative summary is presented in Table 1. Across all settings, MixAR demonstrates consistently strong performance compared to both discrete and continuous AR baselines. Notably, MixAR-L surpasses MAR-H in terms of rFID and achieves a slightly better gFID and IS, despite using nearly half the parameters. This highlights the effectiveness of introducing discrete priors to guide continuous autoregressive modeling, improving fidelity without additional computational burden. When compared to discrete AR models such as LlamaGen-3B and MaskBit,

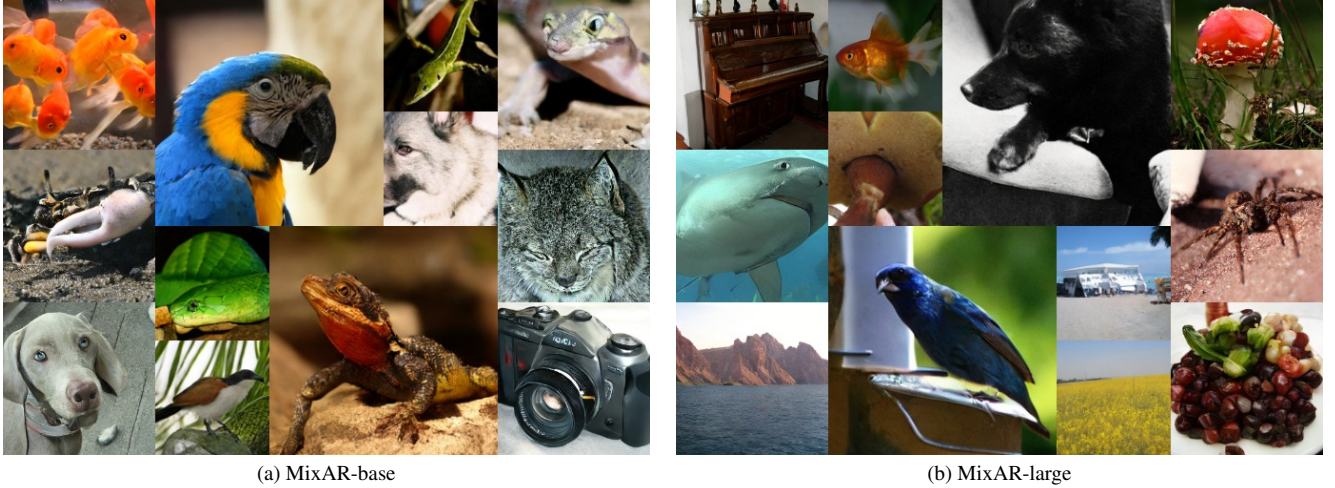


Figure 6. **Qualitative Comparison.** Samples generated by MixAR-base (left) and MixAR-large (right). Our results exhibit high-fidelity textures, consistent global structure and diverse semantics across categories.

Table 1. Quantitative comparisons of Discrete and Continuous AR models on ImageNet-256. Note that the MaskBit results are reproduced under our evaluation protocol.

Method	rFID \downarrow	# Params	gFID \downarrow	IS \uparrow
Discrete AR Models				
VAR-d30-re [22]	1.78	2.0B	1.73	350.2
MaskBit [24]	1.61	305M	1.56	312.3
TiTok	1.71	287M	1.97	281.8
RandAR-XXL	2.19	1.4B	2.15	321.97
MAGVIT-v2	–	307M	1.78	319.4
LlamaGen-3B [19]	0.94	3.1B	2.18	263.3
Continuous AR Models				
HART-d24	0.41	1.0B	2.00	331.5
HART-d30	0.41	2.0B	1.77	330.3
ACDIT-H	1.22	954M	2.37	273.3
MAR-B [13]	1.22	208M	2.31	281.7
MAR-L [13]	1.22	479M	1.78	296.0
MAR-H [13]	1.22	943M	1.55	303.7
Mixture AR Models				
MixAR-B	0.28	208M	1.99	276.96
MixAR-L	0.28	557M	1.53	305.99

MixAR offers substantially lower rFID while maintaining competitive IS scores, demonstrating its ability to capture fine-grained details lost in quantized representations. Moreover, MixAR-B outperforms the similarly sized MAR-B baseline across all metrics, confirming that even lightweight configurations benefit from the proposed mixture formulation. Overall, MixAR achieves a favorable balance between model complexity, fidelity, and efficiency, outperforming larger discrete and continuous counterparts while maintaining parameter efficiency.

Table 2. Efficiency comparison of different guidance mechanisms in the Large model setting with the same backbone and diffusion head.

Method	Inference (sec/img)	Train (min/epoch)	Params (M)
DC-Mix	0.031	39.40	557
DC-SA	0.038	47.28	574
DC-CA	0.037	44.55	707

4.2. Properties of DC-Mix

We implement DC-Mix by replacing the learnable mask-token embedding in MAR with the embeddings of padded discrete tokens extracted from the VQ-VAE codebook. For DC-SA and DC-CA, we follow the standard practice of discrete sequence modeling and use learnable discrete token embeddings. DC-SA injects discrete guidance by prepending discrete tokens as prefix inputs to the continuous sequence, while DC-CA introduces guidance by inserting an additional cross-attention block after every self-attention block in the backbone. Both DC-SA and DC-CA involve 512 tokens, including 256 continuous tokens and 256 discrete ones. In contrast, DC-Mix use 256 mixed tokens with 64 class tokens, reducing the token count by 37.5%. All three variants are built on the same base-size continuous autoregressive backbone, with identical architectural depth (same number of attention blocks) and the same diffusion head. Discrete tokens for both training and inference are obtained using the Maskbit tokenizer and its corresponding generator.

Comparison on efficiency. Table 2 compares the efficiency of different discrete–continuous guidance mecha-

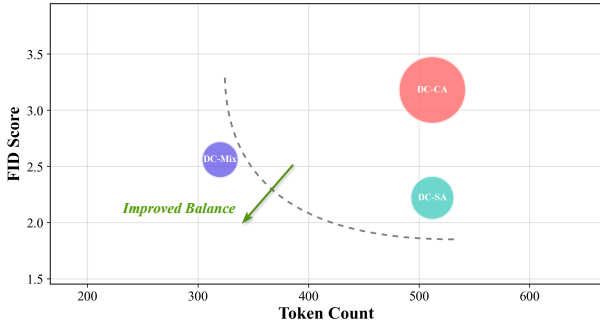


Figure 7. **Balance plot of different guidance strategies.** Our DC-Mix achieve comparable performance with DC-SA while reduce token count by a large portion, achieve an ideal balance between efficiency and fidelity. Both DC-SA and DC-Mix achieve higher generation fidelity (low FID score.)

nisms under the same backbone and diffusion head configuration. Among the three strategies, DC-Mix demonstrates the best overall efficiency, achieving the fastest inference speed (0.031 s/img) and shortest training time (39.40 min/epoch), while using the fewest parameters (557 M). In contrast, DC-SA and DC-CA require additional attention layers to integrate discrete guidance, which increases both computational cost and model size. Specifically, DC-SA adds a modest overhead, while DC-CA incurs the highest cost. Despite these differences, all methods share the same backbone, confirming that the observed efficiency gain stems solely from the simplicity of DC-Mix’s design.

Comparison on the balance of accuracy and efficiency. Figure 7 presents a balance plot comparing different discrete-continuous guidance strategies in terms of FID score versus token count and model size. The token count on the horizontal axis denotes the total number of tokens used for model prediction, including discrete tokens, continuous tokens, and the CLS token. All results are reported after 320 training epochs on ImageNet-256 under identical optimization settings. Among the three variants, DC-Mix achieves a markedly better balance between performance and efficiency. It attains a comparable FID score to DC-SA, while using significantly fewer tokens, and far fewer than DC-CA. This indicates that DC-Mix can retain high generation fidelity while reducing the number of tokens required for autoregressive modeling, thereby improving computational efficiency. The trend shown in the figure highlights that DC-Mix lies closest to the optimal trade-off curve, achieving an ideal balance between model compactness and image quality, whereas DC-SA and DC-CA exhibit diminishing returns with increasing token counts. In practice, if absolute performance is the priority and a higher training cost is acceptable, DC-SA is the most effective choice, as it leverages all tokens for guidance. For computationally constrained

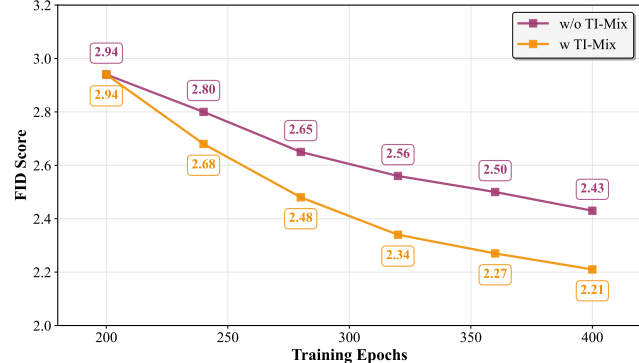


Figure 8. **Ablation Study of TI-Mix.** For model trained with 200 epochs DC-Mix, we continue training with another 200 epochs. Extensive training with TI-Mix significantly outperform with simply increase the training epoch nums.

settings, we recommend DC-Mix, which offers a favorable trade-off between efficiency and fidelity.

4.3. Benefits of TI-Mix

For TI-Mix, we employ a pretrained MaskBit model to generate discrete guidance signals, without introducing any architectural modifications or additional fine-tuning steps. This design choice ensures that TI-Mix can be seamlessly integrated into existing autoregressive pipelines as a plug-and-play enhancement. As illustrated in Figure 8, TI-Mix consistently improves generation fidelity across various training stages. Compared to simply extending training epochs—which often leads to diminishing returns—applying TI-Mix enables the model to better align the training and inference distributions, thereby achieving higher fidelity and more stable convergence. These results demonstrate that incorporating discrete priors through TI-Mix provides a more effective and computationally efficient means of improving continuous autoregressive modeling than prolonged or naive retraining.

5. Conclusion

In this work, we presented MixAR, a unified framework that bridges discrete and continuous autoregressive (AR) modeling through mixture-based training paradigms. By leveraging discrete tokens as prior guidance, MixAR effectively combines the stability of discrete modeling with the expressiveness of continuous latent representations. We explored multiple strategies for integrating discrete and continuous components, including DC-SA, DC-CA, and DC-Mix, and proposed TI-Mix to align the training and inference distributions. Extensive experiments demonstrate that MixAR achieves a strong balance between efficiency and fidelity, and show the improvement to continuous AR models.

Limitations. While MixAR successfully integrates discrete priors into continuous autoregressive frameworks, several limitations remain. The current approach still relies on pretrained discrete tokenizers, which may constrain the representation quality. Future work may explore joint optimization of the tokenizer and AR model, adaptive mixture strategies, and applications to larger-scale multimodal generation tasks.

References

- [1] Josh Achiam, Steven Adler, Sandhini Agarwal, Lama Ahmad, Ilge Akkaya, Florencia Leoni Aleman, Diogo Almeida, Janko Altenschmidt, Sam Altman, Shyamal Anadkat, et al. Gpt-4 technical report. *arXiv preprint arXiv:2303.08774*, 2023. [1](#)
- [2] Imtiaz Ahmed, Sadman Islam, Partha Protim Datta, Imran Kabir, Naseef Ur Rahman Chowdhury, and Ahshanul Haque. Qwen 2.5: A comprehensive review of the leading resource-efficient llm with potential to surpass all competitors. *Authorea Preprints*, 2025. [1](#)
- [3] Victor Besnier, Mickael Chen, David Hurvich, Eduardo Valle, and Matthieu Cord. Halton scheduler for masked generative image transformer. *arXiv preprint arXiv:2503.17076*, 2025. [2, 3](#)
- [4] Tom Brown, Benjamin Mann, Nick Ryder, Melanie Subbiah, Jared D Kaplan, Prafulla Dhariwal, Arvind Neelakantan, Pranav Shyam, Girish Sastry, Amanda Askell, et al. Language models are few-shot learners. *Advances in neural information processing systems*, 33:1877–1901, 2020. [3](#)
- [5] Zhe Cao, Tomas Simon, Shih-En Wei, and Yaser Sheikh. Realtime multi-person 2d pose estimation using part affinity fields. In *Proceedings of the IEEE conference on computer vision and pattern recognition*, pages 7291–7299, 2017. [2](#)
- [6] Huiwen Chang, Han Zhang, Lu Jiang, Ce Liu, and William T Freeman. Maskgit: Masked generative image transformer. In *Proceedings of the IEEE/CVF conference on computer vision and pattern recognition*, pages 11315–11325, 2022. [1, 2, 3](#)
- [7] Jia Deng, Wei Dong, Richard Socher, Li-Jia Li, Kai Li, and Li Fei-Fei. Imagenet: A large-scale hierarchical image database. In *2009 IEEE conference on computer vision and pattern recognition*, pages 248–255. Ieee, 2009. [6](#)
- [8] Jacob Devlin, Ming-Wei Chang, Kenton Lee, and Kristina Toutanova. Bert: Pre-training of deep bidirectional transformers for language understanding. In *Proceedings of the 2019 conference of the North American chapter of the association for computational linguistics: human language technologies, volume 1 (long and short papers)*, pages 4171–4186, 2019. [3](#)
- [9] Abhimanyu Dubey, Abhinav Jauhri, Abhinav Pandey, Abhishek Kadian, Ahmad Al-Dahle, Aiesha Letman, Akhil Mathur, Alan Schelten, Amy Yang, Angela Fan, et al. The llama 3 herd of models. *arXiv e-prints*, pages arXiv–2407, 2024. [1](#)
- [10] Patrick Esser, Robin Rombach, and Bjorn Ommer. Taming transformers for high-resolution image synthesis. In *Proceedings of the IEEE/CVF conference on computer vision and pattern recognition*, pages 12873–12883, 2021. [1, 2, 3](#)
- [11] Doyup Lee, Chiheon Kim, Saehoon Kim, Minsu Cho, and Wook-Shin Han. Autoregressive image generation using residual quantization. In *Proceedings of the IEEE/CVF conference on computer vision and pattern recognition*, pages 11523–11532, 2022. [1](#)
- [12] Tianhong Li, Huiwen Chang, Shlok Mishra, Han Zhang, Dina Katabi, and Dilip Krishnan. Mage: Masked generative encoder to unify representation learning and image synthesis. In *Proceedings of the IEEE/CVF Conference on Computer Vision and Pattern Recognition*, pages 2142–2152, 2023. [1, 2, 3](#)
- [13] Tianhong Li, Yonglong Tian, He Li, Mingyang Deng, and Kaiming He. Autoregressive image generation without vector quantization. *Advances in Neural Information Processing Systems*, 37:56424–56445, 2024. [1, 2, 3, 5, 6, 7](#)
- [14] Aixin Liu, Bei Feng, Bing Xue, Bingxuan Wang, Bochao Wu, Chengda Lu, Chenggang Zhao, Chengqi Deng, Chenyu Zhang, Chong Ruan, et al. Deepseek-v3 technical report. *arXiv preprint arXiv:2412.19437*, 2024. [1](#)
- [15] Fabian Mentzer, David Minnen, Eirikur Agustsson, and Michael Tschannen. Finite scalar quantization: Vq-vae made simple. *arXiv preprint arXiv:2309.15505*, 2023. [1, 3](#)
- [16] Shaoqing Ren, Kaiming He, Ross Girshick, and Jian Sun. Faster r-cnn: Towards real-time object detection with region proposal networks. *Advances in neural information processing systems*, 28, 2015. [2](#)
- [17] Sucheng Ren, Zeyu Wang, Hongru Zhu, Junfei Xiao, Alan Yuille, and Cihang Xie. Rejuvenating image-gpt as strong visual representation learners. *arXiv preprint arXiv:2312.02147*, 2023. [1, 2, 3](#)
- [18] Sucheng Ren, Qihang Yu, Ju He, Xiaohui Shen, Alan Yuille, and Liang-Chieh Chen. Flowar: Scale-wise autoregressive image generation meets flow matching. *arXiv preprint arXiv:2412.15205*, 2024. [3](#)
- [19] Peize Sun, Yi Jiang, Shoufa Chen, Shilong Zhang, Bingyue Peng, Ping Luo, and Zehuan Yuan. Autoregressive model beats diffusion: Llama for scalable image generation. *arXiv preprint arXiv:2406.06525*, 2024. [1, 2, 3, 7](#)
- [20] Yi Sun, Xiaogang Wang, and Xiaou Tang. Deep convolutional network cascade for facial point detection. In *Proceedings of the IEEE conference on computer vision and pattern recognition*, pages 3476–3483, 2013. [2](#)
- [21] Haotian Tang, Yecheng Wu, Shang Yang, Enze Xie, Junsong Chen, Junyu Chen, Zhuoyang Zhang, Han Cai, Yao Lu, and Song Han. Hart: Efficient visual generation with hybrid autoregressive transformer. *arXiv preprint arXiv:2410.10812*, 2024. [3](#)
- [22] Keyu Tian, Yi Jiang, Zehuan Yuan, Bingyue Peng, and Liwei Wang. Visual autoregressive modeling: Scalable image generation via next-scale prediction. *Advances in neural information processing systems*, 37:84839–84865, 2024. [7](#)
- [23] Aaron Van Den Oord, Oriol Vinyals, et al. Neural discrete representation learning. *Advances in neural information processing systems*, 30, 2017. [1, 2, 3](#)
- [24] Mark Weber, Lijun Yu, Qihang Yu, Xueqing Deng, Xiaohui Shen, Daniel Cremers, and Liang-Chieh Chen. Maskbit:

Embedding-free image generation via bit tokens. *arXiv preprint arXiv:2409.16211*, 2024. [1](#), [2](#), [3](#), [5](#), [6](#), [7](#)

[25] Jingfeng Yao, Bin Yang, and Xinggang Wang. Reconstruction vs. generation: Taming optimization dilemma in latent diffusion models. In *Proceedings of the Computer Vision and Pattern Recognition Conference*, pages 15703–15712, 2025. [5](#), [6](#)

[26] Lijun Yu, José Lezama, Nitesh B Gundavarapu, Luca Verzani, Kihyuk Sohn, David Minnen, Yong Cheng, Vighnesh Birodkar, Agrim Gupta, Xiuye Gu, et al. Language model beats diffusion–tokenizer is key to visual generation. *arXiv preprint arXiv:2310.05737*, 2023. [1](#), [3](#)

[27] Qihang Yu, Ju He, Xueqing Deng, Xiaohui Shen, and Liang-Chieh Chen. Randomized autoregressive visual generation. In *Proceedings of the IEEE/CVF International Conference on Computer Vision*, pages 18431–18441, 2025. [1](#)

[28] Zhanpeng Zhang, Ping Luo, Chen Change Loy, and Xiaoou Tang. Facial landmark detection by deep multi-task learning. In *European conference on computer vision*, pages 94–108. Springer, 2014. [2](#)

[29] Yue Zhao, Yuanjun Xiong, and Philipp Krähenbühl. Image and video tokenization with binary spherical quantization. *arXiv preprint arXiv:2406.07548*, 2024. [1](#), [3](#)